

Vietnam Journal of Chemistry, International Edition, **54**(4): 459-466, 2016
 DOI: 10.15625/0866-7144.2016-00347

Synthesis and structural characteristics of platinum(II) complexes with N(4)-substituted thiosemicarbazones

Duong Ba Vu^{1*}, Tran Buu Dang^{1,2}

¹Faculty of Chemistry, Ho Chi Minh City University of Education, Vietnam

²Faculty of Chemistry, Ho Chi Minh City University of Science, Vietnam

Received 7 March 2016; Accepted for publication 12 August 2016

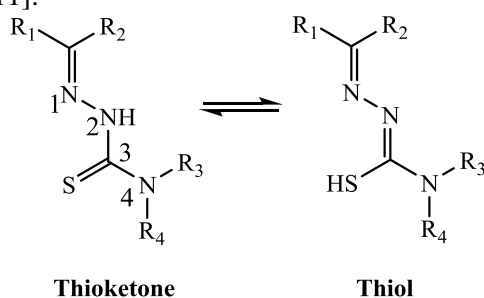
Abstract

Three ligands, namely 4-nitrobenzaldehyde-[N(4)-methyl, N(4)-phenyl thiosemicarbazone] (HL1), fluoren-9-one-[N(4)-(4-methylpiperidinyl)thiosemicarbazone] (HL2), and 4'-hydroxyacetophenone-[N(4)-(4-methylpiperidinyl)thiosemicarbazone] (HL3) as well as three corresponding Pt(II) complexes ([Pt(L)₂](i = 1;2;3)), were synthesized and fully characterized. The analysis of IR, UV-vis, MS, ¹H-NMR, ¹³C-NMR, COSY, and HSQC illustrated that HL1, HL2, HL3 were bidentate ligands and bound to the metal through the imine nitrogen and the net negatively charged sulfur in thiol form. Furthermore, it was demonstrated that the chelating ligands in the Pt(II) complexes were in the *trans* configuration.

Keywords. Thiosemicarbazone, platinum(II) complexes, coordination compounds, inorganic synthesis.

1. INTRODUCTION

Thiosemicarbazone (TSC) ligands are a large group of thiourea derivatives which have attracted much interest due to their antiviral, antimalarial, antifungal, antimicrobial, and antitumor activities [1-11]. In solution state, they can undergo tautomerization to thiol form as depicted in Scheme 1 [4-11].



Scheme 1: The tautomerization of TSC in solution

The conjugated N-N-S tridentate ligand system of TSCs plays an essential role for anticancer activity, as they are reliable to function as prospective inhibitors of ribonucleotide reductase activity [2, 12, 13]. For the reason that TSCs can chelate with trace metals in biological systems, transition metal complexes with N(4)-thiosemicarbazone ligands have also attracted many studies in anticancer therapy as complementary

complexes to those of the well known cisplatin, carboplatin, and oxaliplatin [4-13]. However, among the numerous *d*-metal complexes investigated, only platinum and palladium-based complexes have entered clinical trials due to their useful biological potentials [13]. The anticancer properties of several N(4)-phenyl, N(4)-piperidinyl, or N(4)-cyclohexyl thiosemicarbazone ligands and their corresponding platinum complexes were considerably more effective than other derivatives as well as cisplatin as a result of the N(4)-bulky substituents that influences their lipophilicity [4-12, 14, 15].

In this paper, we describe the preparation and characterization of three TSC ligand derivatives, namely 4-nitrobenzaldehyde-[N(4)-methyl, N(4)-phenyl thiosemicarbazone] (**HL1**), Fluoren-9-one-[N(4)-(4-methylpiperidinyl) thiosemicarbazone] (**HL2**) and 4'-hydroxy acetophenone-[N(4)-(4-methylpiperidinyl)thiosemicarbazone] (**HL3**), along with three of their corresponding Pt(II) complexes: bis-(4-nitrobenzaldehyde-[N(4)-methyl,N(4)-phenylthiosemicarbazone])platinum(II) [**Pt(L1)**]₂, bis-(Fluoren-9-one-[N(4)-(4-methylpiperidinyl)thiosemicarbazone])platinum(II) [**Pt(L2)**]₂, bis-(4'-hydroxyacetophenone-[N(4)-(4-methylpiperidinyl)thiosemicarbazone])platinum(II) [**Pt(L3)**]₂ (Figure 1). The characterization of these ligands and complexes was determined by FTIR,

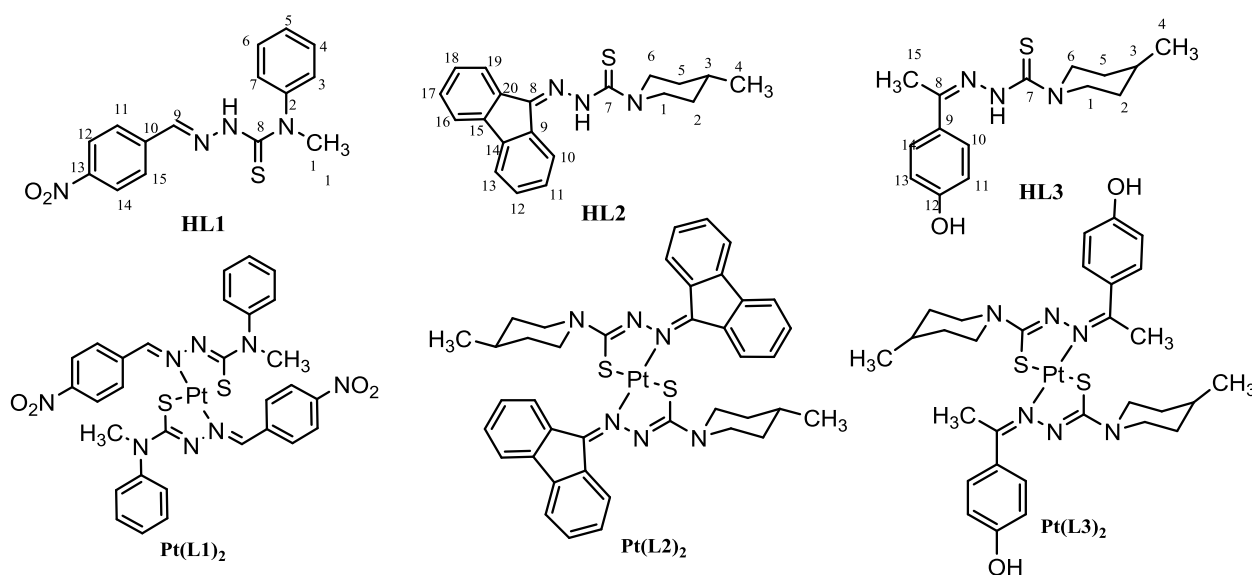
UV-Vis, HRMS, $^1\text{H-NMR}$, $^{13}\text{C-NMR}$, COSY, and HSQC.

Figure 1: Structures of targeted ligands and their corresponding Pt(II) complexes

2. EXPERIMENTAL

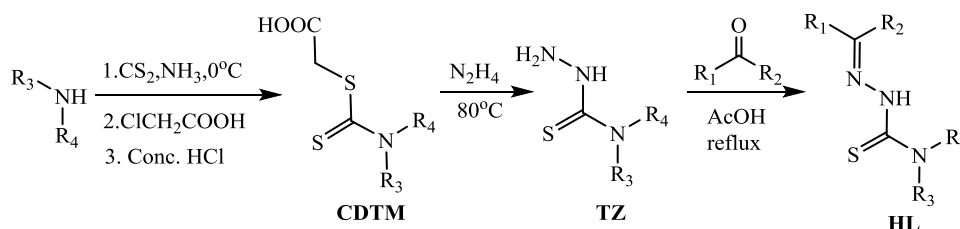
2.1. General

Carbon disulfide, ammonia solution (25%), glacial acetic acid, ethanol (99% purity), platinum wire, nitric acid (63% v/v solution), hydrochloric acid (36% v/v solution), sulfuric acid (98% solution), hydrazine sulfate, 1,4-dioxane, *N,N*-dimethylformamide (DMF), acetone, diethyl ether, potassium chloride, and vaseline were acquired from Guangdong Guanghua Sci-Tech Company, China. *N*-methylaniline (98% purity) and sodium chloroacetate (98% purity) were purchased from Fluka. Fluorene-9-one (99% purity), 4-methylpiperidine (98% purity), 4-nitrobenzaldehyde (98% purity), 4'-hydroxyacetophenone (98% purity), hydrazine hydrate (50-60% purity) were obtained from Merck.

Fourier Transform Infrared (FT-IR) analysis (Shimadzu FT-IR-8400S) was operated in the range of 4000-450 cm^{-1} using compressed KBr pellets. Ultraviolet-visible light absorbance measurements were performed by using a Perkin-Elmer Lambda 25 UV-Vis Spectrometer in the range of 200-700 nm in absolute ethanol. A Gallenkamp MPD-350 was used to determine melting point temperatures. Nuclear magnetic resonance (NMR) spectra were recorded by using a Bruker 500 MHz (in d_6 -dimethylsulfoxide, $\text{DMSO-}d_6$) and high-resolution mass spectrometry positive spectra obtained from a Varian 910 MS.

2.2. Synthesis of ligands

General preparations of TSC ligand derivatives are depicted in scheme 2.



Scheme 2: The synthesis of N(4)-substituted thiosemicarbazones

2.2.1. Preparation of HL

The mixture consisting of *N*-methylaniline or 4-

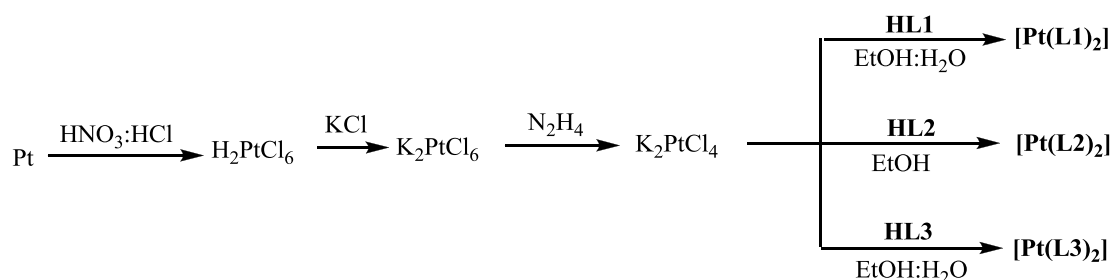
methylpiperidine (0.2 mol) and carbon disulfide (0.2 mol) was treated in 25% NH_3 in the range of 0-10 $^\circ\text{C}$ for 2 h. The filtered yellow precipitate was dissolved

entirely in water, followed by treatment with a saturated solution of $\text{ClCH}_2\text{COONa}$ (0.2 mol) at room temperature for 5 - 6 h. After standing overnight, the yellowish solution was acidified by concentrated HCl . The obtained white solid carboxyl *N*-alkyl dithiocarbamate (**CDTM**) was filtered and recrystallized from ethanol. In the next step, the solution of **CDTM** (0.1 mol) and $\text{N}_2\text{H}_4\cdot\text{H}_2\text{O}$ (0.3 mol) in 10 mL water was heated in the rings of a steam bath in the range of 80-90 °C. When the white *N*-alkyl thiosemicarbazide (**TZ**) was separated, heating was continued for an additional 20 min. **TZ**

(0.01 mol) was re-crystallized from ethanol (or hot water) and then it was experienced with the condensable stage with 4-nitrobenzaldehyde (or 4'-hydroxybenzaldehyde; fluoren-9-one) (0.01 mol) in ethanol/glacial acetic acid prior to filtration and recrystallization.

2.3. Synthesis of complexes

The general preparation of Pt(II) complexes is depicted in scheme 3.



Scheme 3: The synthesis of complexes with the general form, $[\text{Pt}(\text{L})_2]$

2.3.1. Preparation of $\text{K}_2[\text{PtCl}_4]$

Platinum wire (0.05 mol) was shredded and then dissolved in concentrated $\text{HNO}_3:\text{HCl}$ (1:4.5 molar proportion) with slight heating. The removal of excess amount of HNO_3 (and then HCl) occurred by adding HCl solution (and then water) with heating, followed by a reduction in the volume of orange solution containing $\text{H}_2[\text{PtCl}_6]$ to 25 mL. After addition of a saturated KCl solution to the $\text{H}_2[\text{PtCl}_6]$ solution, yellow powder ($\text{K}_2[\text{PtCl}_6]$) was precipitated. This solid was filtered and washed by water and acetone. In the next step, hot $\text{N}_2\text{H}_4\cdot\text{H}_2\text{SO}_4$ (0.01 mol) solution was slowly dropped into 100 mL water containing 0.02 mol of $\text{K}_2[\text{PtCl}_6]$ at 80 °C to obtain red solution $\text{K}_2[\text{PtCl}_4]$. After concentrating this solution, red crystals of $\text{K}_2[\text{PtCl}_4]$ were separated and then filtered and washed by cool water and ethanol (yield: 81%).

2.3.2. Preparation of $[\text{Pt}(\text{L})_2]$

A solution of $\text{K}_2[\text{PtCl}_4]$ (0.24 mmol) and water (10 mL) was slowly dropped into a solution of **HL** (0.48 mmol) dissolved in ethanol (20 mL) at 40 °C. After stirring rigorously for 3-4 h, a solid was precipitated and then filtered and washed by ethanol and diethyl ether.

2.4. Mass analysis of platinum

The percentage of Pt weigh was determined by

the approach based on [16].

3. RESULTS AND DISCUSSION

3.1. HRMS and FT-IR analyses

In HRMS, the spectra of $[\text{Pt}(\text{L})_2]$ exhibited the isotopes of Pt (^{194}Pt , 32.90 %; ^{195}Pt , 33.80 %; ^{196}Pt , 25.30 %; ^{198}Pt , 7.21 %) and S (^{32}S , 95.00 %; ^{33}S , 0.76 %; ^{34}S , 4.20 %) and C (^{12}C , 98.90 %; ^{13}C , 1.1 %), which contributed to the emergence of many subspectra around the parent molecular ion peak. The satisfactory match of predicted molecular mass and *m/z* of molecular ions in HRMS as well as that of predicted and practical %m(Pt) in mass analysis (Table 1) proved all of prepared *bis*-thiosemicarbazone complexes were monomeric structures.

To determine the coordination mode of the TSC ligands with platinum(II), FT-IR data of ligands were compared to those of corresponding complexes as shown in Table 2.

While the stretching vibration of S-H at 2570 cm^{-1} was absent in the IR spectra of the ligands, that of C=S at a range of $1400\text{-}850\text{ cm}^{-1}$ was observed. This indicated that the TSC ligands existed in thioketone form in the solid state. In the IR spectra of the complexes, the absence of the stretching vibrations for N-H, lower shifts in the wavenumbers of C=N and C=S, and an enormous increase in that of N-N illustrated that the tautomerisation taking place led to thiol form in solution. Simultaneously, the

vibration of S-H was not observed in the Pt(II) complexes IR spectra, which involved the deprotonation that the thiol form experienced prior to coordination (Scheme 4) [4-11, 13, 17].

The significant absence of vibrations in the IR spectrum of **[Pt(L2)₂]** provided evidence for its most symmetric structure (figure 2). The square planar **[Pt(L2)₂]** has the identity *E* and a *C₂* axis

perpendicular to σ_h plane through the average planes of two 4-methylpiperidine moieties, which was sufficient enough to adopt an overall symmetry point group of *C_{2h}*. Meanwhile, the vibrations of the functional groups present in **HL1** and **HL3** molecules presented fully in IR spectra of **[Pt(L1)₂]** and **[Pt(L3)₂]**.

Table 1: Results of HRMS and mass analysis

Compound	Formula	<i>m/z</i> [M+1] ⁺	Predicted molecular mass	% m (Pt)	
				Prediction	Experimental
HL1	C ₁₅ H ₁₄ N ₄ SO ₂	315	314	-	-
[Pt(L1)₂]	PtC ₃₀ H ₂₆ N ₈ S ₂ O ₄	822	821	23.75	24.00
HL2	C ₂₀ H ₂₁ N ₃ S	336	335	-	-
[Pt(L2)₂]	PtC ₄₀ H ₄₀ N ₆ S ₂	864	863	22.60	22.73
HL3	C ₁₅ H ₂₁ N ₃ SO	292	291	-	-
[Pt(L3)₂]	PtC ₃₀ H ₄₀ N ₆ S ₂ O ₂	776	775	25.16	24.86

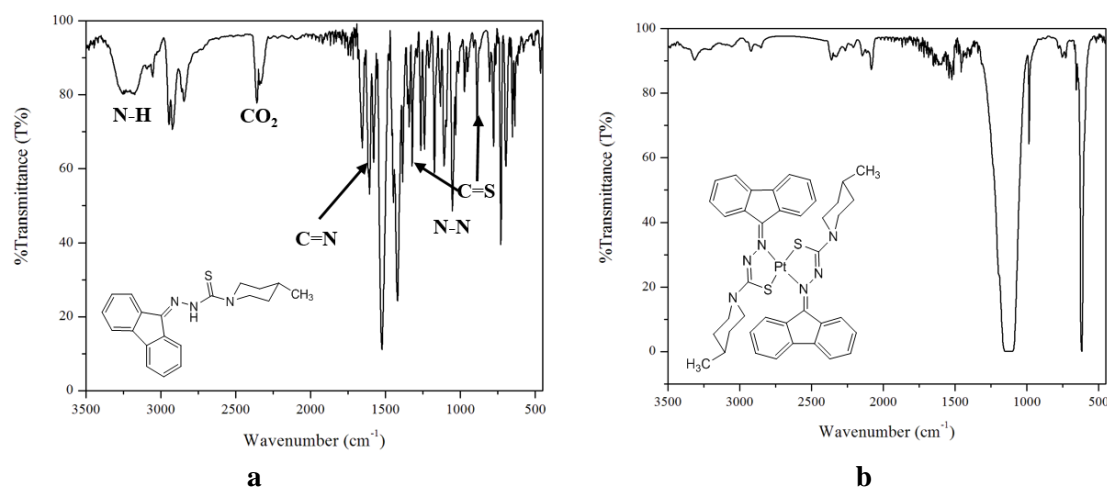
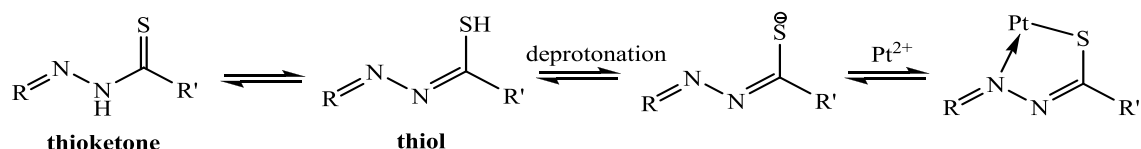


Figure 2: IR spectra of (a) **HL2** and (b) **[Pt(L2)₂]**

Table 2: Relevant FT-IR data of ligands and complexes (all values are quoted in wavenumbers, cm⁻¹)

Compound	$\nu(\text{O-H})$	$\nu(\text{N-H})$	$\nu(\text{C=C(Ar)})$; $\delta(\text{N-H})$; $\nu(\text{-CSNH-})$	$\nu(\text{C=N})$	$\nu(\text{C=S})$	$\nu(\text{N-N})$
HL1	-	3190	1591; 1495; 1451; 1406	1572	1337 924	1024
[Pt(L1)₂]	-	-	1591; 1495; 1449; 1406	1570	1337 924	1040
HL2	-	3196	1605; 1418	1653 1578	1321 889	1030
[Pt(L2)₂]	-	-	-	-	-	1125
HL3	3397	3177	1609	1586	1335 893	1015
[Pt(L3)₂]	3400	-	1609	1593	1325 891	1150



Scheme 4: The coordination mode of thiosemicarbazones

3.3. UV-Vis and NMR analyses

UV-Vis data, provided in table 3, demonstrated additional evidence for the coordination of the TSC ligands with Pt(II). According to the UV-Vis spectrum of $\text{K}_2[\text{PtCl}_4]$ [19], apart from a band at 216 nm (molar absorption coefficient $\epsilon = 10000 \text{ M}^{-1}\cdot\text{cm}^{-1} - \log \epsilon = 4 \text{ M}^{-1}\cdot\text{cm}^{-1}$) assigned to the charge transfer from chloride ion to Pt(II), three absorption bands at 330 nm, 400 nm, and 425 nm with $\log \epsilon < 2 \text{ M}^{-1}\cdot\text{cm}^{-1}$ were assigned to d-d transitions. However, in terms of ligands and complexes, the first band at $200 < \lambda <$

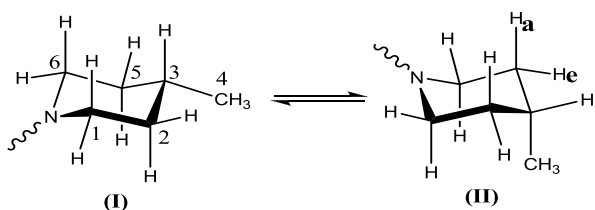
210 nm appeared due to ethanol as a solvent. Other adsorption bands in the range of 230-450 nm with $3.8 < \log \epsilon < 4.6 \text{ M}^{-1}\cdot\text{cm}^{-1}$, were due to $\pi \rightarrow \pi^*$ and $n \rightarrow \pi^*$ transition of the thiosemicarbazone ligand. The band at 330-429 nm was ascribed to $n \rightarrow \pi^*$ transition of azomethine $\text{C}=\text{N}(1)$ and thioamide $\text{N}(2)=\text{CS}$, which noticeably shifted upon complexation with Pt(II) as a result of the newly extended conjugated system. These results clearly demonstrate the chelation of azomethine nitrogen and CS sulfur to Pt(II) [4-11, 13, 19-21].

Table 3: Relevant UV-vis data of ligands and complexes

Compounds	$\pi \rightarrow \pi^*$ ($\lambda/\log \epsilon$)	$n \rightarrow \pi^*$ ($\lambda/\log \epsilon$)	d-d transition ($\lambda/\log \epsilon$)
HL1	255/4.54; 300 ^s	382/4.24	-
[Pt(L1)₂]	255/4.38; 295 ^s	397/4.40	overlapped
HL2	246/4.50; 280 ^s	430/4.02	-
[Pt(L2)₂]	246/4.40; 290 ^s	429/3.81	overlapped
HL3	264/4.33	329/4.76	-
[Pt(L3)₂]	266/4.01	330/4.35	440,00 ^s

s: shoulder.

Our attention then turned to determining the configuration of the free ligands, their coordinated forms, and the conformation of 4-methylpiperidine moiety by NMR analysis. The protons and carbons were numbered according to figure 1. 4-methylpiperidine has two common conformations (scheme 5).



Scheme 5: Equilibrium of two conformations of 4-methylpiperidine

The chemical shifts and characteristics of the observed proton and carbon signals are tabulated in table 4. In ^{13}C -NMR, the relaxation of 4-ordered carbon atom ($\text{C}=\text{S}$) required more time than others, which led to its signal absence after many scans during the investigation. The *E* configuration of **HL1** (around $\text{HC}=\text{N}$) was determined by the

appearance of H9 (8.05 ppm) whereas the *Z* configuration arose $\delta \text{H9} > 8.12 \text{ ppm}$ [21]. The 4-methylpiperidine moiety had the fixed conformation (**I**) because their characteristics of proton and carbon signals matched well to those observed from [19].

Apart from proton-proton coupling, ^{195}Pt can couple to protons in certain positions. The satellite surrounding proton H9 (**[Pt(L1)₂]**) was due to the interaction between ^{195}Pt and protons whose relative distances were the lengths of 3 bonds ($\text{Pt}-\text{N}-\text{C}-\text{H}$) [18]. On the contrary, no satellites were observed in H9 (**HL1**). In **[Pt(L3)₂]**, in spite of $\text{H15}-\text{C}-\text{C}-\text{N}-\text{Pt}$, the satellite of H15 was also observed. This is most likely due to $^{195}\text{Pt}-\text{H15}$ (methyl) spacing interaction, an additional evidence for the *Z* conformation of **HL3** (figure 3). It is noted that the signal of H15 (**HL3**) appeared as a *singlet* in ^1H -NMR. Because of less solubility of **[Pt(L2)₂]** in d^6 -DMSO, the noise overlapped this specific signal, which resulted in loss of these peaks.

Although two ligands bound to platinum in each of the complexes studied, the number of proton signals in the ^1H -NMR spectra was found to be half the total number of protons. Furthermore, small differences in the proton shifts of the ligand and

complex spectra were recorded. Thus, three target complexes were in *trans*-configuration because “*cis*-configuration was not favored due to its steric hindrance from two ligands around the central metal

atom” [17]. These slight differences afforded the small deviation from planarity typically observed in square planar complexes.

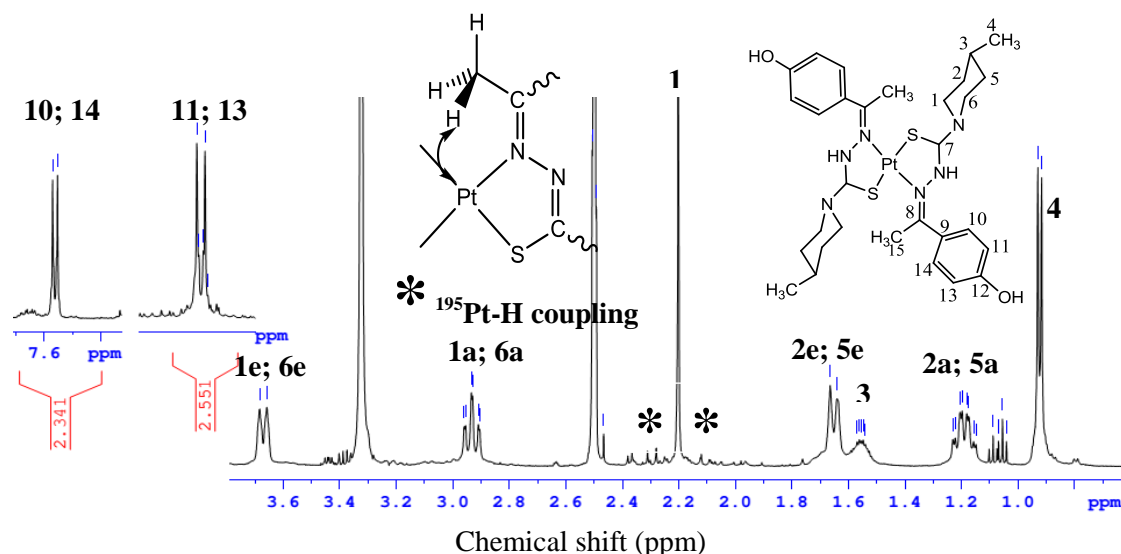


Figure 3: ^1H -NMR spectrum of $[\text{Pt}(\text{L}3)_2]$

Table 4: ^1H -NMR data of ligands and complexes

H	The chemical shift (ppm), coupling constant J (Hz)									
	HL1	$[\text{Pt}(\text{L}1)_2]$	HL2	$[\text{Pt}(\text{L}2)_2]$	HL3	$[\text{Pt}(\text{L}3)_2]$				
1	3.42 (3H,s)	3.43 (3H,s)	H^a	3.00 (2H,t-d) $^3J_{aa} = 12.5$ $^3J_{ae} = 2.5$ $^2J_{gem} = 12.5$	H^a	2.99 (2H,t) $^3J_{aa} = 12.0$ $^2J_{gem} = 12.0$	H^a	2.94 (2H,t-d) $^3J_{aa} = 12.5$ $^3J_{ae} = 2.5$ $^2J_{gem} = 12.5$	H^a	2.93 (2H,t-d) $^3J_{aa} = 12.5$ $^3J_{ae} = 2.5$ $^2J_{gem} = 12.5$
			H^c	3.69 (2H,d) $^2J_{gem} = 12.5$	H^c	3.70 (2H,d) $^2J_{gem} = 12.5$	H^c	3.68 (2H,d) $^2J_{gem} = 13.0$	H^c	3.67 (2H,d) $^2J_{gem} = 13.0$
2	-	-	H^a	1.20 (2H,q-d) $^3J_{aa} = 12.5$ $^3J_{ae} = 4.0$ $^2J_{gem} = 12.5$	H^a	1.22 (2H,t) $^3J_{aa} = 10.0$ $^2J_{gem} = 12.0$	H^a	1.20 (2H, q-d) $^3J_{aa} = 12.0$ $^3J_{ae} = 3.5-4.0$ $^2J_{gem} = 12.5$	H^a	1.18 (2H,q-d) $^3J_{aa} = 12.0$ $^3J_{ae} = 3.5-4.5$ $^2J_{gem} = 12.5$
			H^c	1.67 (2H,d) $^2J_{gem} = 11.0$	H^c	1.68 (2H,d) $^2J_{gem} = 11.0$	H^c	1.66 (2H, d) $^2J_{gem} = 11.0$	H^c	1.65 (2H,d) $^2J_{gem} = 12.0$
3	7.44 (4H,m)	7.46 (4H,m)	1.58 (1H,m)	1.59 (1H,m)	1.56 (1H,m)	1.56 (1H,m)				
4	7.44 (4H,m)	7.46 (4H,m)	0.93 (3H,d) $J = 7.0$	0.94 (3H,d) $J = 6.5$	0.92 (3H,d) $J = 6.5$	0.92 (3H,d) $J = 6.5$				
5	7.29 (1H,t) $J_{ortho} = 6.5$	7.30 (1H,t) $J_{ortho} = 6.5$	H^a	1.20 (2H,q-d) $^3J_{aa} = 12.5$ $^3J_{ae} = 4.0$ $^2J_{gem} = 12.5$	H^a	1.22 (2H,t) $^3J_{aa} = 10.0$ $^2J_{gem} = 12.0$	H^a	1.20 (2H, q-d) $^3J_{aa} = 12.0$ $^3J_{ae} = 3.5-4.0$ $^2J_{gem} = 12.5$	H^a	1.18 (2H,q-d) $^3J_{aa} = 12.0$ $^3J_{ae} = 3.5-4.5$ $^2J_{gem} = 12.5$
			H^c	1.67 (2H,d) $^2J_{gem} = 11.0$	H^c	1.68 (2H,d) $^2J_{gem} = 11.0$	H^c	1.66 (2H, d) $^2J_{gem} = 11.0$	H^c	1.65 (2H,d) $^2J_{gem} = 12.0$

H	The chemical shift (ppm), coupling constant J (Hz)									
	HL1	[Pt(L1) ₂]	HL2		[Pt(L2) ₂]		HL3		[Pt(L3) ₂]	
6	7.44 (4H,m)	7.46 (4H,m)	H ^a	3.00 (2H,t-d) ³ J _{aa} = 12.5 ³ J _{ae} = 2.5 ² J _{gem} = 12.5	H ^a	2.99 (2H,t) ³ J _{aa} = 12.0 ² J _{gem} = 12.0	H ^a	2.94 (2H, t-d) ³ J _{aa} = 12.5 ³ J _{ae} = 2.5 ² J _{gem} = 12.5	H ^a	2.93 (2H,t-d) ³ J _{aa} = 12.5 ³ J _{ae} = 2.5 ² J _{gem} = 12.5
			H ^c	3.69 (2H,d) ² J _{gem} = 12.5	H ^c	3.70 (2H,d) ² J _{gem} = 12.5	H ^c	3.68 (2H,d) ² J _{gem} = 13	H ^c	3.67 (2H,d) ² J _{gem} = 13
7	7.40 (4H, m)	7.46 (4H,m)	-		-		-		-	
8	-	-	-		-		-		-	
9	8.05 (1H,s)	8.07 (1H,s)	-		-		-		-	
10	-	-	7.71 (1H,d); $J = 7.5$		7.71 (1H,d); $J = 7.0$		7.56 (2H,d); $J_{ortho} = 7.5$		7.56 (2H,d); $J_{ortho} = 8.5$	
11	7.77 (2H,d) $J_{ortho} = 9.0$	7.77 (2H,d) $J_{ortho} = 9.0$	7.31 (1H,t-d) $J_{ortho} = 7.5$; $J_{meta} = 1.0$		7.36 (3H,m)		6.76 (2H,d) $J_{ortho} = 9.0$		6.76 (2H,d) $J_{ortho} = 8.5$	
12	8.19 (2H,d) $J_{ortho} = 9.0$	8.19 (2H,d) $J_{ortho} = 9.0$	7.36 (2H,t-d) $J_{ortho} = 7.5$; $J_{meta} = 1.0$		7.36 (3H,m)		-		-	
13	-	-	7.81 (1H,d), $J = 7.0$		7.81 (1H,d), $J = 7.0$		6.76 (2H,d), $J = 9.0$		6.76 (2H,d), $J = 8.5$	
14	8.19 (2H,d) $J_{ortho} = 9.0$	8.19 (2H,d) $J_{ortho} = 9.0$	-		-		7.56 (2H,d) $J_{ortho} = 7.5$		7.56 (2H,d) $J_{ortho} = 8.5$	
15	7.77 (2H,d) $J_{ortho} = 9.0$	7.77 (2H,d) $J_{ortho} = 9.0$	-		-		2.20 (3H,s)		2.20 (3H,s)	
16	-	-	7.85 (1H,d); $J = 7.5$		7.86 (1H,d); $J = 8.0$		-		-	
17	-	-	7.42 (1H,t-d) $J_{ortho} = 7.5$; $J_{meta} = 1.0$		7.42 (1H,t) $J_{ortho} = 7.5$		-		-	
18	-	-	7.36 (2H,t-d) $J_{ortho} = 7.5$; $J_{meta} = 1.0$		7.36 (3H,m)		-		-	
19	-	-	8.64 (1H,d); $J = 7.5$		8.63 (1H,d); $J = 7.5$		-		-	
20	-	-	-		-		-		-	
OH	-	-	-		-		9.65 (1H,s)		9.63 (1H,s)	
NH	12.3 (1H,br)	-	12.3 (1H,br)		-		9.60 (1H, br)		-	

4. CONCLUSION

We have synthesized three N(4)-substituted thiosemicarbazones, namely HL1, HL2, and HL3, and three *trans*-bis-(N(4)-substituted thiosemicarbazone)platinum(II) complexes. The C_{2h} symmetric point group of *trans*-Pt(L2)₂ was evaluated by IR spectrum, whereas others were asymmetric due to their distorted square planar structures. The coordination mode of the ligand with

the metallic action in solution incorporated 3 steps: enolization of thioketone to thiol form (RSH), deprotonation of RSH, and complexation by chelating through azomethine nitrogen and thiomide sulfur. The configuration of *E*-HL1 and *Z*-HL3 as well as fixed-chair conformation of 4-methylpiperidine moiety whose methyl group was at equatorial position remained unchanged in both the free ligands and desired complexes.

REFERENCES

1. D. R. Richardson. *Anti-plasmodial activity of aroylhydrazone and thiosemicarbazone iron chelators: effect on erythrocyte membrane integrity, parasite development and the intracellular labile iron pool*, Inorg. Biochem., **129**, 43-51 (2013).
2. G. Pelosi. *Thiosemicarbazone Metal Complexes: From Structure to Activity*, The Open Crystallography Journal, Vol. 3, 16-28 (2010).
3. D. Kovala-Demertzi, A. Galani, N. Kourkoumelis, J. R. Miller, M.A. Demertzis. *Synthesis, characterization, crystal structure and antiproliferative activity of platinum(II) complexes with 2-acetylpyridine-4-cyclohexyl-thiosemicarbazone*, Polyhedron, **26**, 2871-2879 (2007).
4. P. F. Rapheal, E. Manoj, M.R.P. Kurup, E. Suresh. *Structural and spectral studies of novel Co(III) complexes of N(4)-substituted thiosemicarbazone derived from pyridine-2-carbaldehyde*, Polyhedron, **26**, 607-616 (2007).
5. P. F. Rapheal, E. Manoj, M. R. P. Kurup. *Copper(II) complexes of N(4)-substituted thiosemicarbazones derived from pyridine-2-carbaldehyde: Crystal structure of a binuclear complex*, Polyhedron, **26**, 818-828 (2007).
6. P. F. Rapheal, E. Manoj, M.R.P. Kurup. *Syntheses and EPR spectral studies of manganese(II) complexes derived from pyridine-2-carbaldehyde based N(4)-substituted thiosemicarbazones: Crystal structure of one complex*, Polyhedron, **26**, 5088-5094 (2007).
7. V. Philip, V. Suni, M. R. P. Kurup, M. Nethaji. *Structural and spectral studies of nickel(II) complexes of di-2-pyridyl ketone N,N-(butane-1,4-diyl) thiosemicarbazone*, Polyhedron, **23**, 1225-1233 (2004).
8. V. Philip, V. Suni, M. R. P. Kurup, M. Nethaji. *Novel binuclear copper(II) complexes of di-2-pyridyl ketone N(4)-methyl, N(4)-phenylthiosemicarbazone: structural and spectral investigations*, Polyhedron, **24**, 1133-1142 (2005).
9. V. Philip, V. Suni, M. R. P. Kurup, M. Nethaji. *Manganese(II) complexes of substituted di-2-pyridyl ketone thiosemicarbazones: structural and spectral studies*, Spectrochimica Acta Part A, **64**, 171-177 (2006).
10. V. Philip, V. Suni, M. R. P. Kurup, M. Nethaji. *Copper(II) complexes derived from di-2-pyridyl ketone N(4),N(4)-(butane-1,4-diyl)thiosemicarbazone: crystal structure and spectral studies*, Polyhedron, **25**, 1931-1938 (2006).
11. K. Alomar, A. Landreau, M. Allain, G. Bouet, G. Larcher, *Synthesis, structure and antifungal activity of thiophene-2,3-dicarboxaldehyde bis(thiosemicarbazone) and nickel(II), copper(II) and cadmium(II) complexes: unsymmetrical coordination mode of nickel complex*, Inorg. Biochem., **126**, 76-83 (2013).
12. K. Hu, z. Yang, S. Pan, H. Xu, J. Ren. *Synthesis and antitumor activity of liquiritigenin thiosemicarbazone derivatives*, Med. Chem., **45**, 3453-3458 (2010).
13. D. Palanimuthu, A.G. Samuelson. *Dinuclear zinc bis(thiosemicarbazone) complexes: Synthesis, in vitro anticancer activity, cellular uptake and DNA interaction study*, Inorg. Chim. Acta., **408**, 152-161 (2013).
14. N. M. Samus, V. I. Tsapkov, A. P. Gulya. *Coordination compounds of cobalt, nickel, copper and zinc with thiosemicarbazone and 3-phenylpropenal semicarbazone*, Russ. J. Gen. Chem., **74**, 1428 (2004).
15. Sarmistha Halder, Ray J. Butcher, Samaresh Bhattachayra. *Synthesis, structure and spectroscopic properties of some thiosemicarbazone complexes of platinum*, Polyheron, **26**, 2741-2748 (2007).
16. T. T. Da, N. H. Dinh. *Coordination compounds–Synthesis and Structural Analysis*, Science and Technology Publishing House, Hanoi, 149 (2007).
17. M. S. Bakkar, M. Yamin Siddiqi, M. S. Monshi. *Preparation and investigation of the bonding mode in the complexes of Pt(II) with thiosemicarbazone ligands*, Synth. React. Inorg. Met-Org Chem., **33**, 1157-1169 (2003).
18. T. T. Da, D. B. Vu, N. H. Dinh. *Synthesis and structure of some mixed cis-diamine complexes of platinum(II) containing morpholine and another amine*, Coord. Chem., **57**, 485-496 (2006).
19. D. B. Vu, T. B. Dang. *Synthesizing N(4)-substituted thiosemicarbazones and their structural characteristics*, HCMUP Journal of Science, **5**, 12-19 (2014).
20. D. T. Quang, V. D. Do, C. D. Kinh. *UV-Vis spectra of some Platinum(II) complexes with thiosemicabazonate ligands*, Vietnam Journal of Chemistry, Vol. 43, 322-325 (2005).
21. W. Hernandez, J. Paz, A. Vaisberg, E. Spodine, R. Richter, L. Bayer. *Synthesis, characterization, and in vitro cytotoxic activities of benzaldehyde thiosemicarbazone derivatives and their palladium(II) and Platinum(II) complexes against various human tumor cell lines*, Bioorg. Chem. and App., 2008, 1-9 (2008).

Corresponding author: **Duong Ba Vu**

Faculty of Chemistry, Ho Chi Minh City University of Pedagogy
280 An Duong Vuong Street, District 5, Ho Chi Minh City,
E-mail: vudb@humup.edu.vn; Tel.: 090 936 0909.